Available online at www.sciencedirect.com
SCIENCE DIRECT
Journal of Power Sources 144 (2005) 208–213
JOURNAL OF POWER SOURCES
www.elsevier.com/locate/jpowsour

Short communication

Lithium insertion chemistry of phosphate phases with the lipscombite structure

Mickael Dollé, Sébastien Patoux, Thomas J. Richardson *

Environmental Energy Technologies Division, Lawrence Berkeley National Laboratory, Berkeley, CA 94720, USA

Received 18 November 2004; accepted 15 December 2004
Available online 19 February 2005

Abstract

The lithium insertion chemistry of an iron phosphate with the lipscombite structure, $Fe_{1.19}PO_4F_{0.11}(OH)_{0.46}(H_2O)_{0.43}$, was investigated by X-ray diffraction (XRD), galvanostatic cycling, and potentiostatic intermittent titration. The compound, prepared by a simple hydrothermal method, contains interconnecting chains of face-sharing FeO_6 octahedra with about 60% Fe occupancy. Assuming that all the iron may be reduced, the theoretical capacity is about 180 mAh g^{-1}, similar to that of olivine-type $LiFePO_4$. Reversible intercalation was found to proceed via a single-phase reaction at an average potential of 2.8 V versus Li^+/Li. Good structural stability upon intercalation/deintercalation was observed. The unit cell volume increased linearly and isotropically with increasing lithium content, reaching 10% for a Li:Fe ratio of 0.96. XRD peak widths increased on lithiation, presumably due to disorder created by conversion of Fe^{3+} to the larger Fe^{2+}, but decreased on subsequent delithiation. The rate capability of this material appears to be diffusion-limited, and may benefit from a decrease in particle size. The lithium insertion behavior of a related compound, $Ti_5O_4(PO_4)_4$, was also investigated.

Keywords: Lithium batteries; Iron phosphate; Intercalation compounds

1. Introduction

In recent years, considerable attention has been devoted to complex oxides containing three-dimensional polyanion frameworks such as olivine-type $LiFePO_4$ and NaSiCON-type $Li_3Fe_2(PO_4)_3$, built of MO_6 octahedra and $(XO_4)^{n-}$ tetrahedra, for use as positive electrodes in rechargeable lithium batteries [1–4]. Although these compounds have somewhat lower theoretical capacities than simple oxides, the strongly bonded $(XO_4)^{n-}$ units confer exceptional stability and safety. $LiFePO_4$ has been the most studied, presenting a flat voltage plateau at about 3.4 V versus Li/Li^+, associated with the Fe^{3+}/Fe^{2+} couple, but it has some kinetic limitations due to the two-phase $LiFePO_4/FePO_4$ system and the limited electronic conductivity of both phases. Significant improvements in rate capability have been achieved by coating the oxide particles with carbon by physical or chemical means [5,6] and by decreasing the particle size [7]. Hydrated iron phosphates and their dehydrated derivatives [8,9] have generated some interest, but these compounds, too, require carbon coating to overcome their poor electronic conductivity. Materials with composition $[Li,Na]_2[Fe,Mn]_3(PO_4)_3$, having the alluaudite structure, were found to remain single-phase during Li insertion, but exhibited poor capacities [10]. Here we report the structural and electrochemical characteristics of the hydrated iron phosphate fluoride $Fe_{1.19}PO_4[F_{0.11}(OH)_{0.46}(H_2O)_{0.43}]$, having the structure of lipscombite ($Fe_{1.5}PO_4OH$) [11]. In this material (Fig. 1), slightly distorted FeO_6 octahedra share faces to form chains that are connected to other chains by corner sharing. These structural features could enhance the compound's electronic conductivity relative to that of the highly insulating olivine, $LiFePO_4$, in which FeO_6 units share only corners. Moreover, if Li intercalation proceeds via a single-phase in which a mixture of iron oxidation states is present, the conductivity may be greater,

* Corresponding author. Tel.: +1 510 486 8619; fax: +1 510 486 8619.
E-mail address: tjrichardson@lbl.gov (T.J. Richardson).

0378-7753/$ – see front matter © 2005 Elsevier B.V. All rights reserved.
doi:10.1016/j.jpowsour.2004.12.028

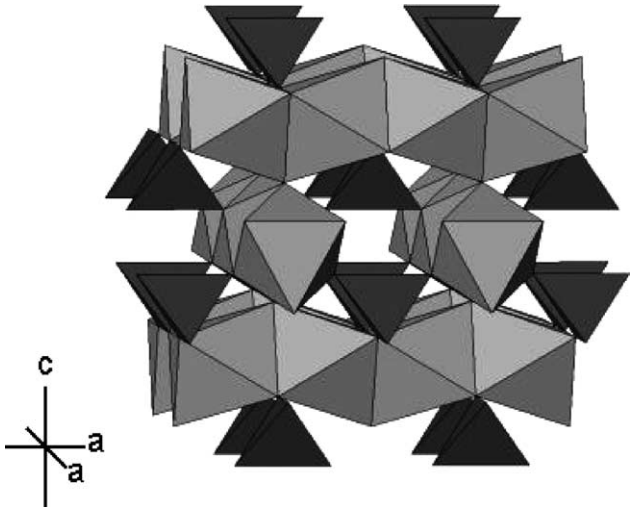

Fig. 1. Structure of $Fe_{1.19}PO_4F_{0.11}(OH)_{0.46}(H_2O)_{0.43}$ showing FeO_6 octahedra (grey) and PO_4 tetrahedra (black).

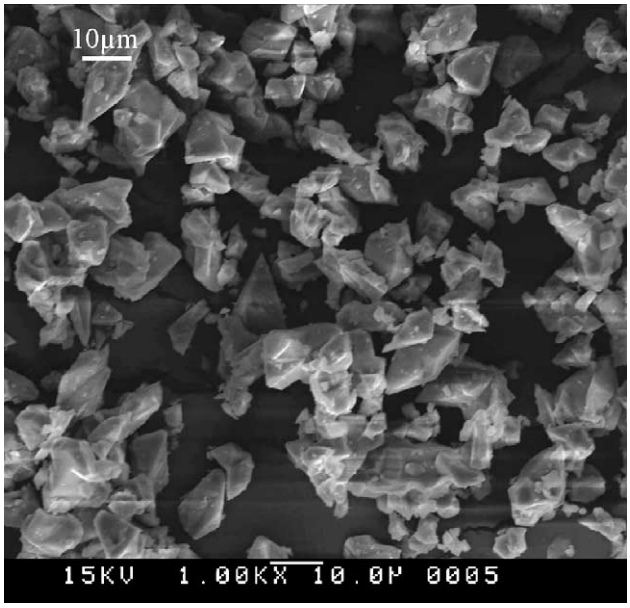

Fig. 2. Scanning electron micrograph of $Fe_{1.19}PO_4F_{0.11}(OH)_{0.46}(H_2O)_{0.43}$ particles.

and the activation energy for rearrangement of the structure may be lower. As prepared, all iron atoms in $Fe_{1.19}PO_4$-$[F_{0.11}(OH)_{0.46}(H_2O)_{0.43}]$ are in the oxidized (+3, high spin) state, leading to a theoretical capacity of 180 mAh g^{-1} if all iron atoms can be reduced and sufficient sites for Li insertion are available. Here we discuss the electrochemical performance of this material in lithium cells and the structural changes observed during cycling.

2. Experimental

The synthesis was carried out hydrothermally as reported by Loiseau et al. [11]. A mixture of $Fe(NO_3)_3{\cdot}9H_2O$, P_2O_5, NH_4HF_2, and H_2O in the molar ratio 1:1:1:40 was held at 200 °C for 6 days in a 60 ml Teflon-lined stainless steel reactor (Parr Co., Moline, IL). The resulting pale brown powder was washed several times with distilled water and dried at room temperature. The sample consisted of well-formed cubo-octahedral crystallites (Fig. 2) about 5 μm in size. XRD patterns were obtained using a Siemens D500 diffractometer with monochromatic Cu $K\alpha_1$ radiation ($\lambda = 1.54056$ Å). The programs FULLPROF [12] and RIQAS (MDI Inc., Livermore, CA) were used for Rietveld refinement by whole pattern fitting. The XRD pattern (Fig. 3) showed it to be single-phase with $a = 5.181(1)$ Å and $c = 13.020(8)$ Å, in good agreement with Ref. [11]. Elemental composition was determined by inductively coupled plasma (ICP) atomic absorption analysis (Luvak Inc., Boylston, MA).

$Ti_5O_4(PO_4)_4$ was prepared as follows: titanium isopropoxide was mixed with an excess of 1 M H_3PO_4, producing a white precipitate which was first dried at 60 °C and then heated at 900 °C for 12 h. The resulting white powder was characterized by XRD as $Ti_5O_4(PO_4)_4$ with a small TiP_2O_7 impurity. Rietveld refinement in the $P2_12_12_1$ space group gave $a = 12.804(2)$ Å, $b = 14.426(3)$ Å and $c = 7.479(2)$ Å, in good agreement with those reported from single crystal data [13].

Electrodes were prepared by thoroughly mixing the well-ground phosphates (70.4 wt.%) with 12.4 wt.% carbon black (Shawinigan black) and 17.2 wt.% poly(vinylidenedifluoride) in a 6 wt.% NMP solution. The mixture was applied to aluminum foil by the doctor blade method. The electrodes were dried overnight at ambient temperature and then for 12 h at 60 °C in vacuum. Coin cells were assembled in an argon-filled glove box using Celgard 3401 separators, $LiPF_6$ (1 M) in ethylene

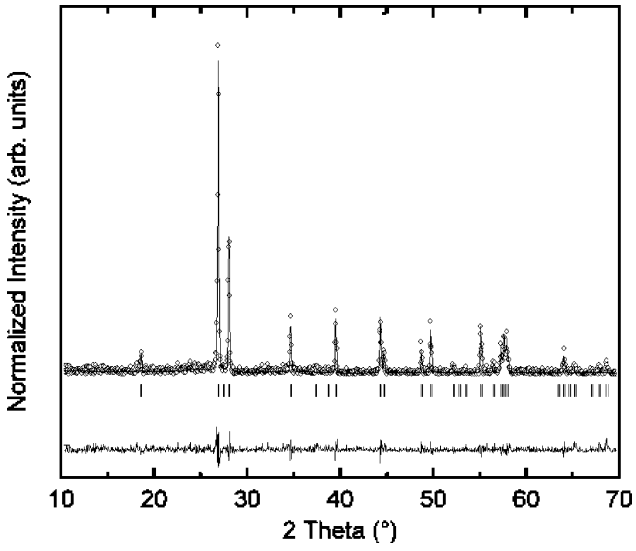

Fig. 3. XRD pattern refinement of $Fe_{1.19}PO_4F_{0.11}(OH)_{0.46}(H_2O)_{0.43}$: open circles represent experimental data points, upper solid line denotes calculated pattern, lower solid line represents the difference, vertical bars indicate the locations of reflections.

carbonate/dimethyl carbonate (1:2, w/w) (Selectipur®, Merck, Darmstadt, Germany) and Li foil (Cyprus-Foote Mineral Co., Kings Mountain, NC) as negative electrode. The cells were cycled between 2.0 V and either 4.1 or 4.5 V at different rates using an Arbin battery test system (Arbin Inc., College Station, TX). Potentiostatic intermittent titration was performed using a MacPile II (Bio-Logic, SA, Claix, France) potentiostat/galvanostat.

3. Results and discussion

3.1. Structural characterization and elemental analysis

The lipscombite structure is built up from $Fe_2O_4X_2$ ($X = F^-, OH^-$ or H_2O) octahedra and PO_4 tetrahedra (Fig. 1). The octahedra share faces and form infinite straight chains along [1 0 0] at $z = 1/4$ and 3/4,and along [0 1 0] at $z = 0$ and 1/2. The chains are interconnected by both X ions and PO_4 tetrahedra. Only about 60% of the Fe sites are occupied, with short-range ordering of vacancies. Loiseau et al. [11] prepared a material by the same method with composition $Fe_{1.21}PO_4F_{0.45}(OH)_{0.18}(H_2O)_{0.37}$, and showed using Mössbauer spectroscopy that all iron ions were in the +3 state. The composition of our sample, hereinafter referred to as FPX, was found to be $Fe_{1.19}PO_4F_{0.11}(OH)_{0.46}(H_2O)_{0.43}$.

3.2. Charge–discharge cycling

The electrochemical behavior of FPX upon lithium insertion at a rate corresponding to ca. *C*/10 is presented in Fig. 4. During the first discharge to 2.0 V, 0.7 Li ions per formula unit were taken up (105 mAh g^{-1}). On the following charge, only 0.56 lithium could be extracted, giving a reversible capacity for the first cycle of 84 mAh g^{-1}. The potential–composition curve is sigmoidal, with an average potential of 2.8 V, slightly lower than that reported for the amorphous and crystalline forms of $FePO_4{\cdot}2H_2O$ [9]. In the case of ball-milled $FePO_4{\cdot}2H_2O$, however, only 10% of the theoretical capacity was obtained, as compared to 59% for hand-ground FPX. This could be due to greater electronic conductivity in FPX, or to a smaller irreversible loss of lithium due to the lower water content. The discharge capacity increased steadily during the first 30 cycles (Fig. 4, inset), equalling the first discharge after 80 cycles. Similar behavior was reported [9] for $FePO_4{\cdot}2H_2O$ and attributed to "electrochemical grinding" of the particles as they expand and shrink upon insertion–deinsertion.

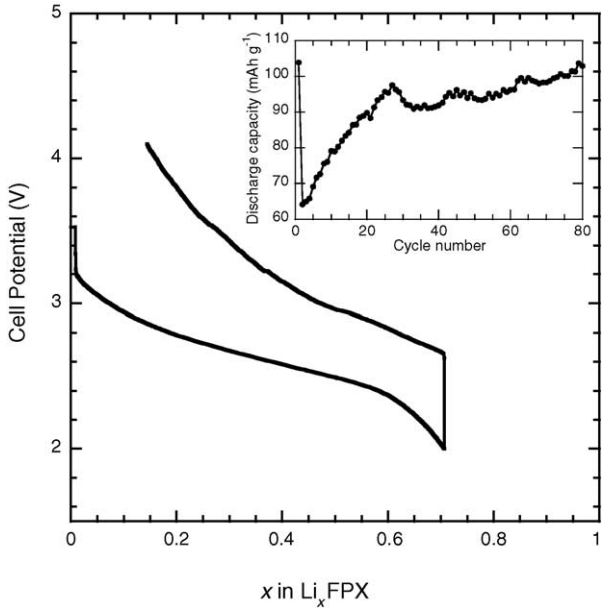

Fig. 4. Potential vs. composition for first discharge and charge for FPX/Li cell. Inset: discharge capacity vs. cycle number.

3.3. Potentiostatic intermittent titration

Although FPX did not require carbon coating, it exhibited some kinetic limitations. The potentiostatic intermittent titration technique (PITT) can provide information about diffusion in a single solid solution domain [14]. An FPX electrode was first activated by galvanostatic cycling at a *C*/10 rate between 2 and 4.5 V versus Li^+/Li. PITT measurements were carried out by applying increasing potential steps of 10 mV between 2 and 4.45 V and measuring the current as a function of time. When the current decreased to *C*/50, the potential was stepped to the next level. The procedure was repeated for decreasing potentials. The voltage and current data are plotted as a function of composition in Fig. 5. The absence of the bell-shaped current response that is characteristic of a two-phase reaction indicates that Li_xFPX exists as a single-phase within this composition range. From the monotonic behavior of the current, it is clear that the reaction is diffusion-controlled. The exponential current decay after an initial rapid increase following each potential step follows

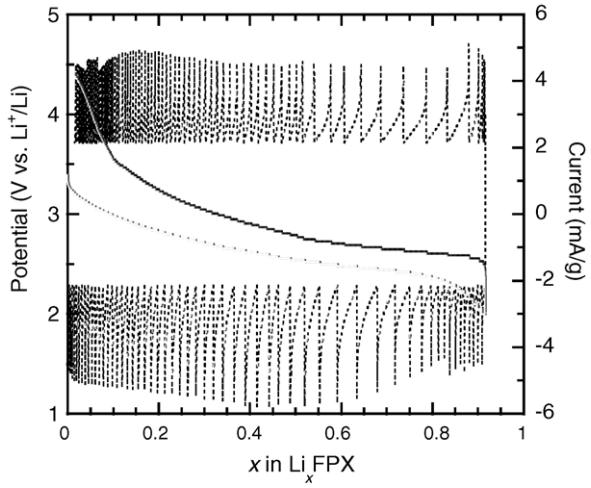

Fig. 5. Chronoamperometric response (dashed line) of the second potentiodynamic cycle (solid line) of FPX/Li cell with10 mV potential steps.

the form [15]:

$$I(t) = \frac{2FS(C_S - C_0)\tilde{D}}{L} \exp\left[-\frac{\pi^2 \tilde{D}t}{4L^2}\right], \quad \text{when } t \gg \frac{L^2}{\tilde{D}} \tag{1}$$

where F is the Faraday constant, S the electrochemically active area, L the diffusion length (set equal to half of the average particle size of 5 μm), and $(C_S - C_0)$ represents the change in Li concentration at the positive electrode–electrolyte interface. To accurately determine diffusion coefficients, an experiment was performed using a limiting current of $C/300$. The values of $\tilde{D}$ were on the order of 10^{-12} cm^2 s^{-1}, quite high compared with those (10^{-14} to 10^{-16} cm^2 s^{-1}) measured for $LiFePO_4$ and $FePO_4$ [16], and of the same order of magnitude as those reported for $LiCoO_2$ [14].

3.4. Structural evolution during Li insertion/extraction

To investigate the phase stability of FPX upon cycling, we undertook an ex situ study of the XRD pattern evolution as a function of state of charge (SOC). A 20 mm × 25 mm electrode was discharged and charged in a beaker cell containing 1 M $LiClO_4$ in propylene carbonate at 20 μA cm^{-2} for varying periods, washed to remove electrolyte, removed from the glove box, and mounted in the diffractometer. The evolution of the XRD pattern is shown in Fig. 6. The tetragonal symmetry was preserved during cycling and no new phases appeared. The unit cell expanded on lithiation (Table 1), and contracted on subsequent delithiation, with some hysteresis. The Fe–O bond lengths (Fig. 7) increased from an average of 2.03 Å in the fully oxidized state ($x = 0$) to 2.18 Å in $Li_{1.00}$ FPX. Using an ionic radius of 1.38 for O^{2-}, the ionic radii of the Fe ions in the two compounds are 0.65 and 0.80 Å, respectively, consistent with the tabulated values of 0.65 and 0.78 Å for high spin Fe^{3+} and Fe^{2+} [17]. The average Fe–O bond lengths in olivine $FePO_4$ and $LiFePO_4$ are 2.10 and 2.16 Å, respectively. The much greater changes in FPX reflect its less rigid structure, which allows accommodation of Fe ions of different sizes and a gradual transition between oxidized and reduced forms in a single-phase system.

Table 1
Open-circuit potentials, cell parameters, and apparent crystallite sizes for $Li_xFe_{1.19}PO_4F_{0.11}(OH)_{0.46}(H_2O)_{0.43}$ at different states of charge

x	OCP (V)	a (Å)	c (Å)	V (Å^3)	Crystallite size (nm)
0.00	3.40	5.1799(3)	13.019(2)	349.3	38
0.76	2.70	5.2676(9)	13.123(7)	364.1	10
1.14	2.60	5.305(1)	13.285(9)	373.8	7
0.63	3.35	5.2265(4)	12.945(3)	353.6	24
0.30	3.50	5.2250(3)	12.896(3)	352.1	26
1.00	2.40	5.366(2)	13.465(9)	387.8	6

During the first discharge, some Li was taken up irreversibly, possibly due to reduction of water and/or ion exchange of Li for protons. The development of lattice parameters and other structural characteristics on subsequent cycles were reversible, as shown in Fig. 8, where cell volume and apparent crystallite size are plotted as a function of open-

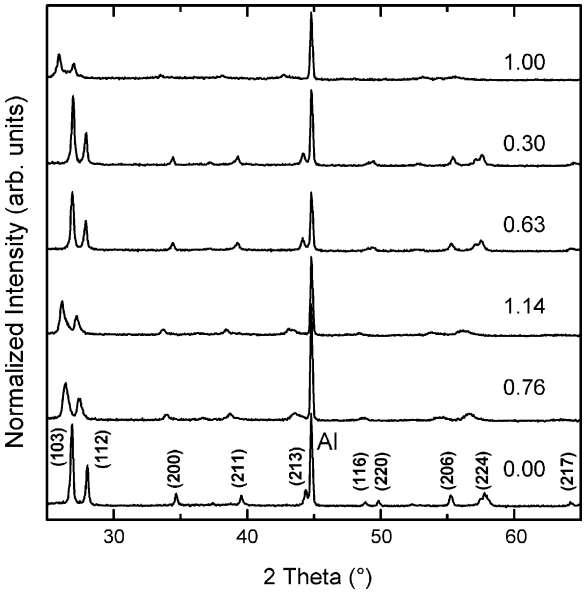

Fig. 6. Evolution of ex situ XRD patterns of FPX electrode. Numbers on right indicate the value of x in Li_xFPX.

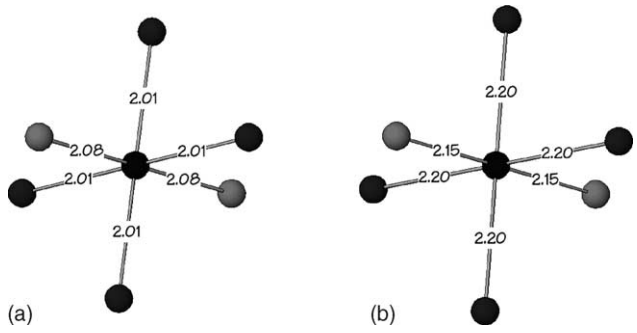

Fig. 7. FeO_6 coordination in (a) FPX and (b) $Li_{1.00}FPX$.

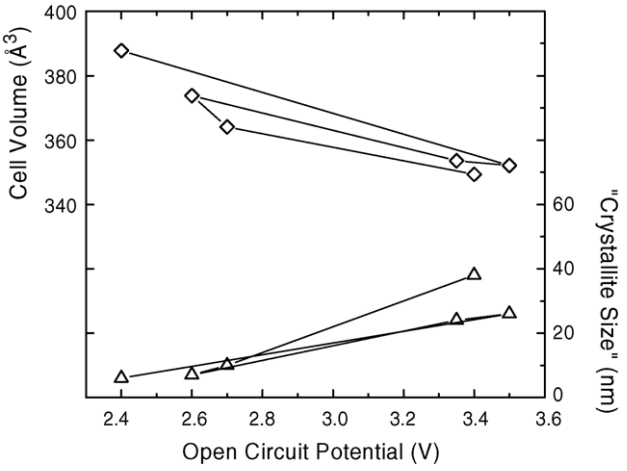

Fig. 8. Unit cell volume and apparent crystallite size vs. open-circuit potential of FPX electrode.

circuit potential rather than Li content. The apparent crystallite size (as determined from the widths of the diffraction peaks) decreased steadily as Li was inserted but increased on subsequent Li extraction. This may be attributed to stress or disorder induced by the much greater increase in the equatorial Fe–O bond lengths during lithiation than in the axial bond lengths. Although there was a large volume expansion on lithiation, it was nearly isotropic, and "electrochemical grinding" is considered unlikely to occur in this material. The structure of the parent compound readily accommodates Fe^{3+}, but must endure some distortion during the conversion to Fe^{2+}.

3.5. Other compounds with the lipscombite structure

A number of compounds have the lipscombite structure with differing occupancy of the MO_6 units. Most of them contain water and/or hydroxide as in $Fe_{1.5}PO_4OH$ and $V_{0.94}Co_{0.46}PO_4(OH)_{0.74}(H_2O)_{0.26}$ [18]. The preparation of water-free compounds is more difficult, but β-Fe_2OPO_4 [19] and $Ti_5O_4(PO_4)_4$ [13] are known examples. In β-Fe_2OPO_4, all the octahedra are occupied, but only half of the iron ions are in the +3 state leading to a theoretical capacity of only 120 mAh g^{-1}. In the case of $Ti_5O_4(PO_4)_4$, five-eighths of the octahedra are occupied and all Ti is in the +4 state, giving a theoretical capacity of about 190 mAh g^{-1}. A $Ti_5O_4(PO_4)_4$/Li cell (Fig. 9) displayed a first discharge capacity of 160 mAh g^{-1}, with two plateaux distinguishable at about 2.0 and 1.6 V versus Li^+/Li. The TiP_2O_7 impurity, whose behavior is characterised by plateaux at 2.63 and 2.57 V versus Li^+/Li [20], did not appear to be electrochemically active in these cells, presumably due to its poor electronic conductivity, which cannot be enhanced by simple hand-grinding with carbon. The cells were cycled between 1.2 and 4.0 V at a *C*/20 rate. Subsequent discharge curves had a similar shape with lower capacities on both plateaux but the total held steady at 80 mAh g^{-1} (Fig. 9, inset). These results confirm the good cycling stability of compounds with the lipscombite structure, but the limited capacities and large first cycle irreversibility (50%) are significant drawbacks.

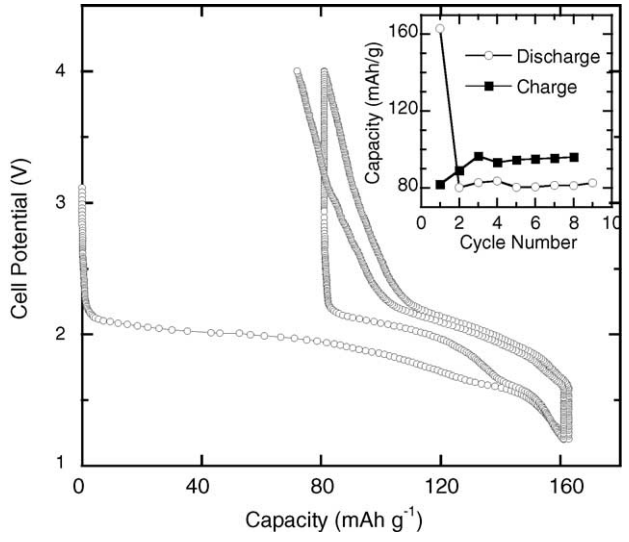

Fig. 9. Potential vs. composition for the two first cycles of $Ti_5O_4(PO_4)_4$/Li cell. Inset: charge and discharge capacity vs. cycle number.

4. Conclusions

Lipscombite-type $Fe_{1.19}PO_4F_{0.11}(OH)_{0.46}(H_2O)_{0.43}$ is an easily prepared Fe^{3+} host for reversible Li insertion in non-aqueous electrolytes, with a sloping discharge potential averaging 2.8 V versus Li. The material remains single-phase over the range of 0 to 1.14 Li atoms per formula unit. The capacity at low rates is about 120 mAh g^{-1}. Its high rate performance is hindered by a slow diffusion process and by the large particle size resulting from the hydrothermal synthesis, and may be improved by grinding or shorter preparation times. The presence of water in the structure results in some excess discharge capacity that is not recovered on the first charge, but on repeated cycling, perhaps due to gradual ion exchange, the discharge capacity increases steadily. Development of a solid state synthetic route, like that for $Ti_5O_4(PO_4)_4$, to reduce the water content and to substitute other transition elements for iron in this structure are in progress.

Acknowledgment

This work was supported by the Assistant Secretary for Energy Efficiency and Renewable Energy, Office of FreedomCAR and Vehicle Technologies of the U.S. Department of Energy under Contract No. DE-AC03-76SF00098.

References

[1] C. Delmas, A. Nadiri, J.L. Soubeyroux, Solid State Ionics 28 (1988) 419.
[2] K.S. Nanjundaswamy, A.K. Padhi, J.B. Goodenough, S. Okada, H. Ohtsuka, H. Arai, J. Yamaki, Solid State Ionics 92 (1996) 1.
[3] C. Masquelier, A.K. Padhi, K.S. Nanjundaswamy, J.B. Goodenough, J. Solid State Chem. 135 (1998) 228.
[4] A.K. Padhi, K.S. Nanjundaswamy, J.B. Goodenough, J. Electrochem. Soc. 144 (1997) 1188.
[5] N. Ravet, Y. Chouinard, J.F. Magnan, S. Besner, M. Gauthier, M. Armand, J. Power Sources 97 (2001) 503.
[6] M.M. Doeff, Y.Q. Hu, F. McLarnon, R. Kostecki, Electrochem. Solid State Lett. 6 (2003) 207.
[7] P.P. Prosini, M. Carewska, S. Scaccia, P. Wisniewski, M. Pasquali, Electrochim. Acta 48 (2003) 4205.
[8] P.P. Prosini, M. Lisi, S. Scaccia, M. Carewska, F. Cardellini, M. Pasquali, J. Electrochem. Soc. 149 (2002) 297.
[9] C. Masquelier, P. Reale, C. Wurm, M. Morcrette, L. Dupont, D. Larcher, J. Electrochem. Soc. 149 (2002) 1037.
[10] T.J. Richardson, J. Power Sources 119 (2003) 262.
[11] T. Loiseau, P. Lacorre, Y. Calage, J.M. Grenèche, G. Férey, J. Solid State Chem. 105 (1993) 417.

[12] J. Rodriguez-Carvajal, FULLPROF: a program for Rietveld refinement and pattern matching analysis, in: Abstracts of the Satellite Meeting on Powder Diffraction of the 15th Congress of the IUCr, Toulouse, France, 1990, p. 127.
[13] F. Reinauer, R. Glaum, Acta Crystallogr. B 54 (1998) 722.
[14] Y.-I. Yang, B.J. Neudecker, N.J. Dudney, Electrochem. Solid State Lett. 4 (2001) 74.
[15] C.J. Wen, B.A. Boukamp, R.A. Huggins, W. Weppner, J. Electrochem. Soc. 126 (1979) 2258.
[16] P.P. Prosini, M. Lisi, D. Zane, M. Pasquali, Solid State Ionics 148 (2002) 45.
[17] R.D. Shannon, Acta Crystallogr. A 32 (1976) 751.
[18] E. Le Fur, A. Riou, O. Pena, J.Y. Pivan, Solid State Sci. 2 (2000) 135.
[19] M. Ijjaali, B. Malamam, C. Gleitzer, K. Warmer, J.A. Hriljac, A.K. Cheetham, J. Solid State Chem. 86 (1990) 195.
[20] S. Patoux, C. Masquelier, Chem. Mater. 14 (2002) 5057.